Resonant Long-Wave Run-Up On A Plane Beach

Themistoklis Stefanakis, Frédéric Dias, Denys Dutykh

Resonant Long-Wave Run-Up On A Plane Beach

T. S. Stefanakis[1,2], F. Dias[2,1] & D. Dutykh[3]

[1] CMLA, Ecole Normale Supérieure de Cachan, Cachan cedex, France

[2] School of Mathematical Sciences, University College Dublin, Dublin, Ireland

[3] LAMA, Université de Savoie, Le Bourget-du-Lac, France

ABSTRACT

Even though wave run-up is not a new subject, until recently analytical and numerical studies of long wave run-up on a plane beach have failed to identify the existence of resonant regimes. Furthermore, it was a common belief that the leading wave will result in the maximum run-up. Stefanakis et al. (2011) underlined the importance of resonant long wave interactions during run-up and run-down. In the current paper we provide additional results with the use of one-dimensional numerical simulations in the framework of the nonlinear shallow water equations with boundary forcing for plane and nontrivial beaches. Several wave profiles are used as forcing conditions to the boundary value problem. Resonant interactions between incident and receding waves are found to occur, depending on the beach slope and the wavelength, and result in enhanced run-up of non-leading waves.

KEY WORDS: Long wave; run-up; resonance.

INTRODUCTION

From a mathematical standpoint, wave run-up, which is the maximum vertical extent of wave uprush on a beach above still water level (Sorensen, 1997), has an intrinsic difficulty: the moving shoreline. The no-slip condition applied at the initial shoreline for the solution of the Navier-Stokes equations, implies that the shoreline should remain stationary, which of course is not the case. Despite this difficulty, major progress to the solution of the initial value problem in one propagation direction was achieved with the introduction of the Carrier and Greenspan (CG) transformation (1958), which allows the reduction of the two nonlinear shallow water equations (NSWE) into a single linear equation and the transformation of the moving wet/dry interface to a stationary point. Further important advances on the subject were achieved by Keller and Keller (1964), Carrier (1966) and Synolakis (1987), with the latter deriving an analytical expression for the run-up of solitary waves. The solitary wave together with the N-wave (Tadepalli and Synolakis, 1994) are the two predominant conceptual wave profiles in tsunami literature, even though more recent studies (Madsen et al., 2008, Madsen and Shaffer, 2010) question them and propose more geophysically relevant paradigms. Expressions for long wave run-up that are independent of the incident wave profile were derived by Didenkulova and Pelinovsky (2008). All the above studies dealt with the initial value problem (IVP). Antuono and Brocchini (2007) solved the boundary value problem (BVP) for the NSWE, using the CG transformation, and applied a perturbation approach by assuming small amplitude incoming waves at the seaward boundary. Later, the same authors (2010) solved the BVP in physical space without use of the CG transformation.

The only ones who addressed the two-dimensional problem were Brocchini and Peregrine (1996). They used a transformation to relate the longshore coordinate to the time variable. This operation allowed the derivation of an expression for the horizontal velocity, which reduced the dimensions and transformed their problem into the already solved one-dimensional canonical problem. However, their solution is only valid for mild angles of incidence.

Almost all of the aforementioned studies focus on the value of maximum wave run-up. Nevertheless, none of these theoretical models is able to capture extreme values such as those observed during the Java 2006 tsunami (Fritz et al., 2007). Moreover, despite the fact that solitary waves or N-waves might be appropriate as models for the leading tsunami waves, DART buoy measurements reveal a sequence of waves reaching the shore. Furthermore, it has been reported that in some cases it is not the leading wave that caused the maximum damage. Scientists explain this phenomenon by assuming that the amplification is due to reflection and refraction effects from nearshore topographic features (Neetu et al., 2011) or due to earthquake-generated local submarine landslides. It is found that bathymetric changes may lead to wave resonance (Kajiura, 1977; Agnon and Mei, 1988; Grataloup and Mei, 2003). In addition, shelf resonance (Munk et al., 1964; Rabinovich and Leviant, 1992), responsible for wave amplification phenomena, is caused due to trapping of long waves on the continental shelf region, which requires the existence of a shelf break (i.e. abrupt change of bathymetry). This type of resonance is observed when the incident wavelength is four times larger than the continental shelf and is found to affect tides as well as tsunamis. However, shelf resonance, as stated above, mainly describes wave amplification and not run-up amplification. In the present study we shed light on the run-up amplification phenomenon by non-leading long waves with the use of one-dimensional numerical simulations of the NSWE for the boundary value problem. Our solver uses a Finite Volume Characteristic Flux scheme with a UNO2 type of reconstruction for higher order terms and a third order Runge-Kutta

time discretization. The model is described in detail and validated by Dutykh et al. (2011a).

WAVES ON A PLANE BEACH

Monochromatic Waves

The maximum wave run-up for the geometry of Fig. 1 was first studied for three different beach slopes, namely, tanθ = 0.13, 0.26, and 0.3, using incident monochromatic waves at the seaward boundary (x = -L) of the form:

$$\eta(-L,t) = \pm\eta_0 \sin(\omega t), \quad \omega / \sqrt{g \tan(\theta)/L} \in (0, 6.29) \qquad (1)$$

where η(x,t) is the free-surface elevation, ω is the angular frequency, θ is the beach angle and g is the gravitational acceleration. At the seaward boundary, we only prescribe the free-surface elevation and not the velocity because boundary velocity is actually a result of the BVP as pointed out by Antuono and Brocchini (2010). However, in our opinion, the realistic implementation of the seaward boundary conditions still remains a open question and one should also keep in mind that the NSWE are an approximate model.

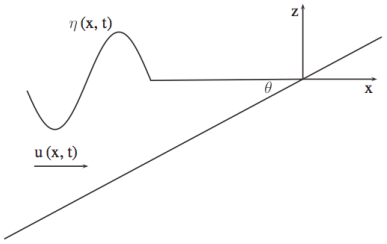

Fig. 1: Schematic of run-up problem geometry.

The maximum run-up was found to depend on the incident wavelength, the beach slope as well as the beach length (Fig. 2). For a given slope, the maximum run-up is highest when the non-dimensional wavelength $\lambda_0/L \approx 5.1$ (i.e. at L = 1000 m offshore, the resonant wavelength is $\lambda_0 =$ 5100 m) for which resonance is observed. Here λ_0 denotes the wavelength of the incident wave:

$$\lambda_0 = \frac{2\pi\sqrt{gL\tan(\theta)}}{\omega} \qquad (2)$$

The maximum run-up increases with increasing slope and with increasing beach length and the run-up amplification reaches values that are extremely high ($R_{max}/\eta_0 \approx 60$). Increasing the beach length leads to an observation of a secondary resonant regime at $\lambda_0/L = 1.5$ (Fig. 2). Resonant amplification is apparent in both leading elevation and leading depression waves. Adding dispersion to the system (Dutykh et al., 2011a) results in reduced amplification values, though without qualitatively changing the overall picture, as the resonant frequencies remain the same. The resonant maximum run-up values are not achieved by the first incident wave, as is the case for $\lambda_0/L > 10$, but by subsequent ones (Fig. 3), which strengthens the assumption of the existence of a resonant mechanism between incident and receding waves. Linear theory (Pelinovsky and Mazova, 1992) does not predict resonant regimes, according to which $R_{max}/\eta_0 = 2\pi\ (2L/\ \lambda_0)^{1/2}$. Our numerical results are in close agreement with linear theory for non-resonant regimes (Fig. 2).

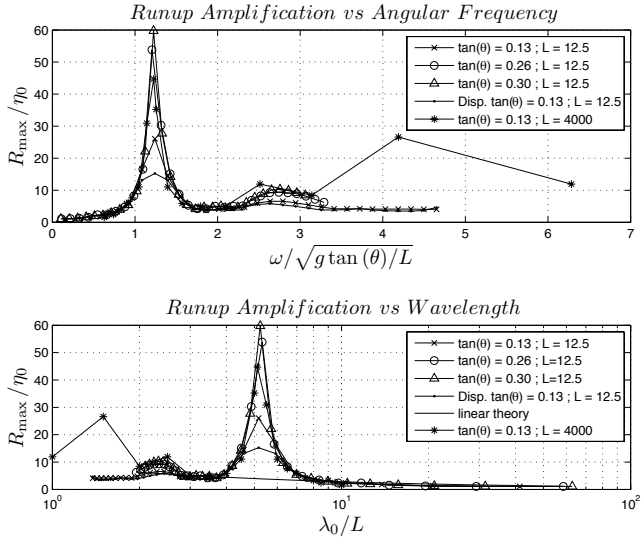

Fig. 2: Maximum run-up amplification factor as a function of non-dimensional angular frequency (top) and non-dimensional wavelength (bottom) for two beach lengths (L = 12.5 m and 4000 m).

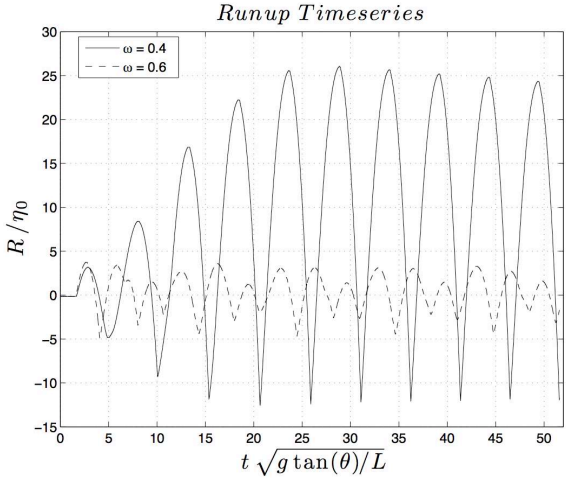

Fig. 3: Run-up timeseries for two different angular frequencies, namely ω = 0.4 s^{-1}, which is the resonant frequency when tanθ = 0.13 and ω = 0.6 s^{-1}, which is a non-resonant frequency for the same slope (L = 12.5 m).

In Fig. 3 we can observe that waves with both resonant and non-resonant frequencies reach a quasiperiodic state of equilibrium, although non-resonant frequencies reach this state faster. A differentiating point is the existence of a single peak (trough) [run-up (run-down)] at the quasiperiodic state of the resonant frequency, while the non-resonant frequencies show multiple peaks (troughs). This difference indicates the synchronization between the incident and reflected waves on the run-up and run-down process in the resonant regime.

The spatiotemporal behaviour of the non-dimensional horizontal velocity is shown in Fig. 4. From this figure we can observe that during the resonant run-up (Fig. 4a) in one location there is an abrupt change

from negative to high positive values of the velocity, which clearly states the creation of a wave front. On the other hand, the run-down process is much smoother but during it the wave assumes higher absolute velocities than during the run-up. In the same figure it can be seen that the velocity in inundated areas does not go to zero as the shoreline recedes. This is due to the presence of a very thin layer of fluid ($h/\eta_0 < 10^{-2}$) which recedes very slowly and is not considered in the computation of the shoreline position. The non-resonant regime exhibits velocities that do not vary as much over time and are lower than the equivalent resonant ones (Fig. 4b).

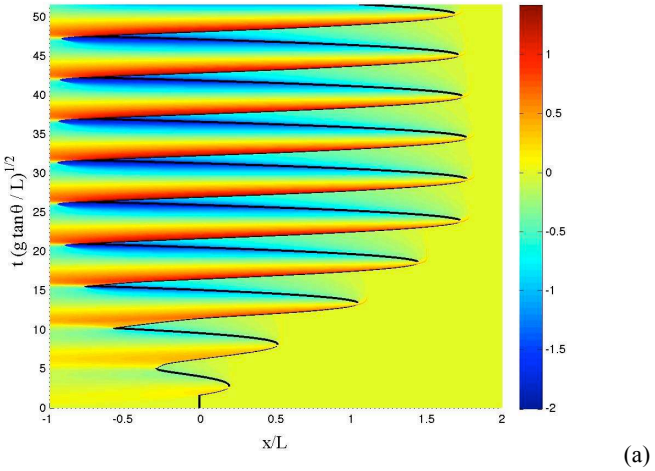

(a)

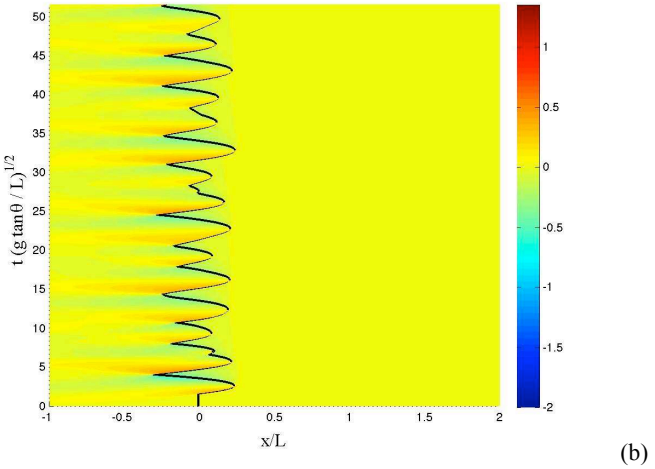

(b)

Fig. 4: Spatiotemporal behaviour of non-dimensional horizontal velocity u / (g tanθ L)$^{1/2}$ in the resonant regime (a) and non-resonant regime (b). The black line describes the evolution of the shoreline position in time. In both cases tanθ = 0.13 and L = 12.5 m.

The resonant run-up mechanism is now examined in terms of energy. The potential and kinetic energy are respectively (Dutykh and Dias, 2009):

$$E_P = \frac{1}{2}\rho g \int_x \eta^2 \, dx \qquad (3)$$

$$E_K = \frac{1}{2}\rho \int_x \int_{-h}^{\eta} u^2 \, dx dz \qquad (4)$$

The energy evolution for the resonant regime when tanθ = 0.3 is depicted in Fig. 5. Both maximum potential and kinetic energies increase over time until a quasiperiodic state is reached. The potential energy takes its maximum value at the instance of maximum run-up, when the kinetic energy is minimum. Moreover, the maximum potential energy is approximately 5 times larger than the equivalent kinetic energy. The extreme oscillations in the total energy are due to the large volumetric changes (inflow-outflow) during run-up and run-down (Fig. 6), which actually affect the limits of integration in the energy equations. Since the volume of fluid inside the computational domain is changing, the current resonant mechanism should not be confused with wavemaker resonance (inside a laboratory flume the volume remains constant).

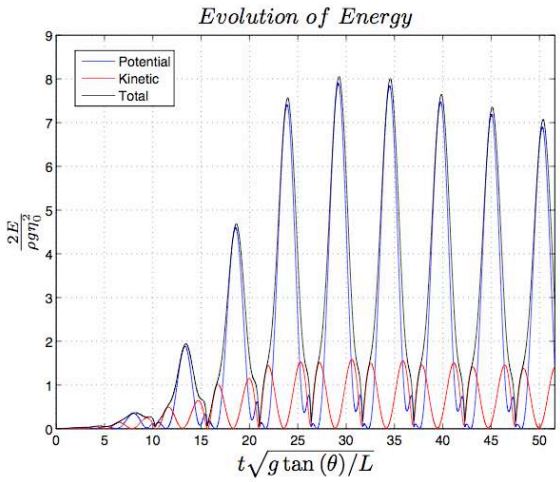

Fig. 5: Energy evolution for the resonant regime ($\omega = 0.6\ s^{-1}$) when tanθ = 0.3 and L = 12.5 .

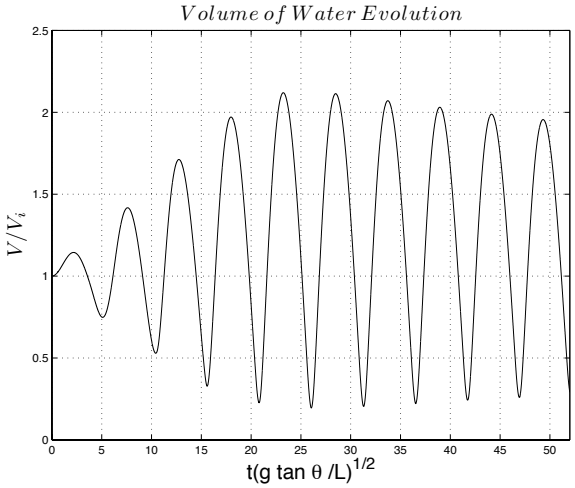

Fig. 6: Evolution of the volume of water inside the computational domain. V_i is the initial volume.

Bichromatic Waves

In order to further explore whether there is more physics carried out by modal interactions in the resonant run-up amplification phenomenon,

we investigated waves of bichromatic modal structure. In order to make direct comparisons with the monochromatic case, each mode had half the amplitude of the equivalent monochromatic wave ($\eta_0/2$). According to our simulations (Fig. 7) no important new interactions are found to occur. When one of the two frequencies is in the resonant regime, the run-up is dominated by this frequency, while the second (non-resonant) frequency does not interfere in the dynamics. When both frequencies are resonant, there is a little enhancement of the run-up but it is not very significant. Nevertheless, an important finding is that the resonant mechanism is not restricted to the monochromatic wave case.

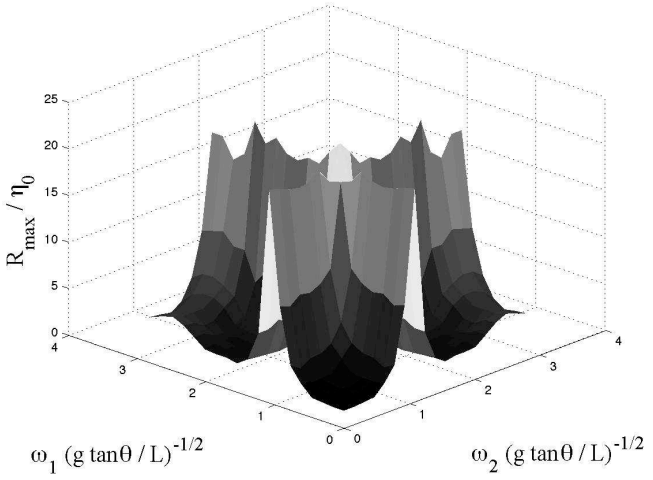

Fig. 7: Maximum run-up of a dichromatic wave as a function of non-dimensional frequency when tanθ = 0.13 and L = 12.5 .

Cnoidal Waves

Cnoidal wave profiles were also investigated as boundary forcing:

$$\left.\begin{aligned} \eta(-L,t) &= \eta_0 - H\ sn^2\left(\frac{kc\,t}{2},m\right) \\ kc &= \left(\frac{3g}{mh}\right) \\ H &= \frac{\eta_0 m K}{K-E} \end{aligned}\right\} \quad (5)$$

where sn is a Jacobian elliptic function with parameter m (0<m<1), and K=K(m) and E=E(m) are the complete elliptic integrals of the first and second kind, respectively (Abramowitz and Stegun, 1965). The parameter m controls both the wave profile and the wavelength. Small m values result in high frequency sinusoidal waves, whereas high m values tend to solitary-like wave profiles. These cnoidal waves are exact solutions to the nonlinear Serre equations (Serre, 1953; Dias and Milewski, 2010). Varying the parameter m, the maximum run-up shows a more complex behaviour (Fig. 8) compared to monochromatic waves. Multiple resonant regimes, interrupted by "calmer" ones, are observed, the severity of which grows with increasing m. The run-up amplification reaches the value R_{max}/η_0 = 27 which clearly is considerably high.

Single Wave With Tail

All previous simulations dealt with idealized wave conditions. However, we wanted to explore whether similar resonant phenomena can occur during a real tsunami. For this reason, a simulation was run for the 25 October 2010 Mentawai Islands tsunami. A virtual wave

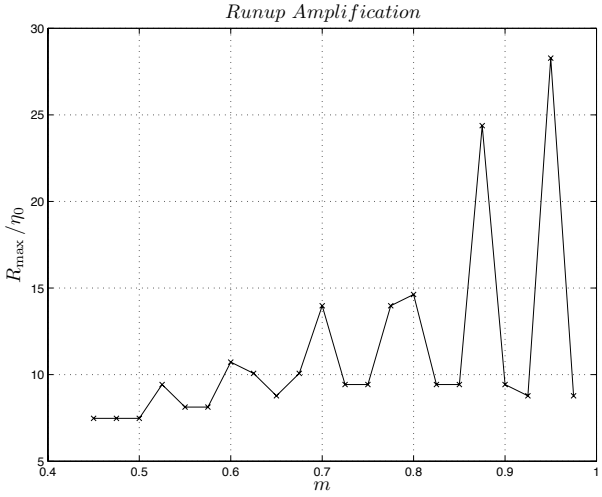

Fig. 8: Cnoidal run-up amplification as a function of parameter m.

gauge was placed at Lon = 100.24^o E, Lat = -3.4^o N which recorded the free-surface elevation timeseries for the first 10,800 s of the tsunami (Fig. 9a). At the wave gauge location, the depth is approximately 120 m. Therefore the mean actual slope to the closest shore is tanθ = 0.03. Using this slope and by setting the first 2000 s of the gauge recordings as boundary forcing, we computed the evolution of the shoreline elevation (Fig. 9b). We can observe the run-up of three waves at t = 720 s, t = 1320 s, and t = 1860 s. It is clear that the first wave does not lead to the highest run-up, even though it has the highest amplitude, as recorded by the wave gauge. Therefore, local resonant tsunami run-up amplification might give an explanation to why it is not always the leading higher wave that causes the maximum damage.

WAVES ON A NON-TRIVIAL BEACH

Driven by our curiosity to see whether our results can be extended to real bathymetries, we ran simulations of monochromatic waves over a transect of the real Mentawai bathymetry (Fig 10a). The existence of multiple resonant peaks may be observed in Fig. 10b. However, the run-up amplification is not as high as in the plane beach case. Nevertheless, the existence of several resonant regimes implies that in nature this phenomenon might not be rare.

CONCLUSIONS

In summary, we discovered local resonant run-up amplification phenomena demonstrated in the context of the one-dimensional BVP of NSWE on a plane beach. The resonance occurs due to the interaction between incoming and reflected waves, and the actual amplification ratio depends on the beach slope and beach length for the case of monochromatic waves. Resonant wave interactions are apparent for various idealized wave profiles, such as dichromatic and cnoidal waves.

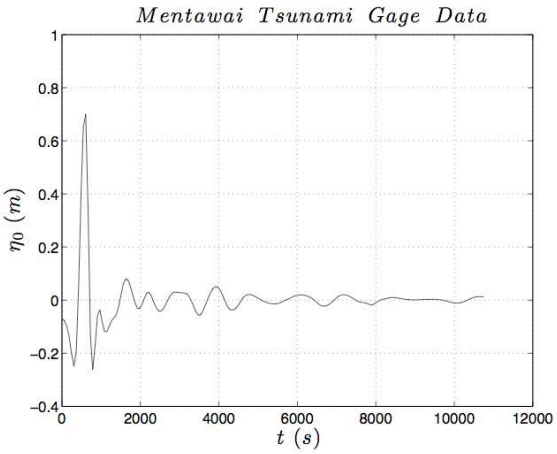

(a)

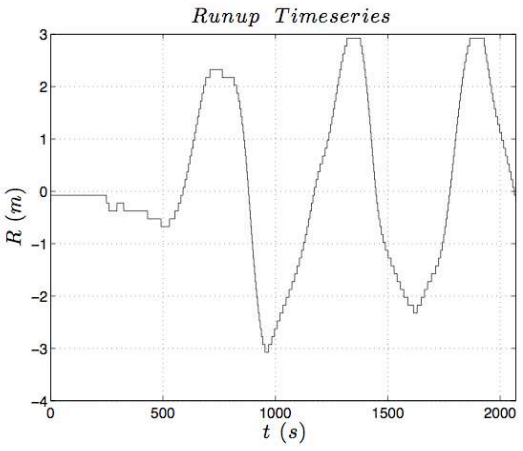

(b)

Fig. 9: (a) Virtual wave gauge recordings (Lon = 100.24° E, Lat = -3.4° N) for the 25 October 2010 Mentawai Islands tsunami. (b) Evolution of the shoreline elevation for the first 2000 s.

These phenomena can explain why it is not always the first wave that results in the highest run-up. More realistic wave profiles, which are typical of tsunamis can also exhibit resonant behaviour, explaining why the tail of a single wave may produce leading-order run-up values. Resonant mechanisms are not limited to the plane beach paradigm but can be observed in more complex bathymetries, as well, thus suggesting that local run-up amplification is not a rare event. However, when the bathymetry is non-trivial, we cannot draw firm conclusions on what extent resonance is attributed to wave trapping and generation of harmonics. Moreover, further research should be conducted on the relevance of the run-up amplification mechanism to the continental shelf resonance (Munk et al., 1964; Rabinovich and Leviant, 1992). We will also investigate resonant long-wave run-up on two-dimensional bathymetry, with the VOLNA code (Dutykh et al., 2011b).

ACKNOWLEDGEMENTS

We would like to acknowledge Professors C. C. Mei and C. E. Synolakis for insightful discussions. This work has been partially supported by the Strategic and Major Initiatives scheme of University College Dublin and by the Framework Program for Research, Technological Development, and Innovation of the Cyprus Research Promotion Foundation under the Project ΑΣΤΙ/0308(BE)/05.

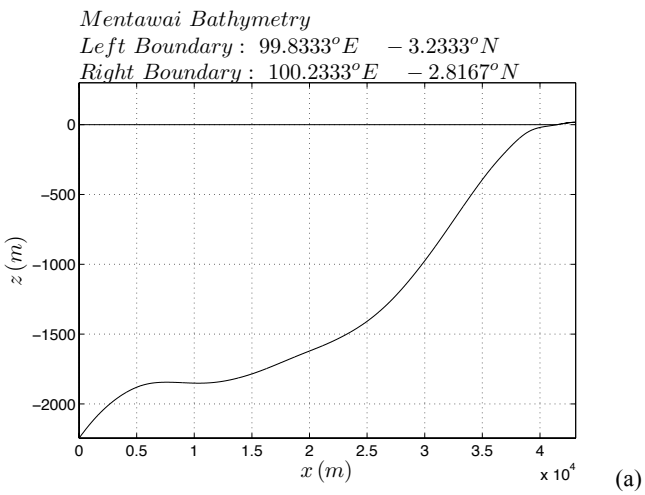

(a)

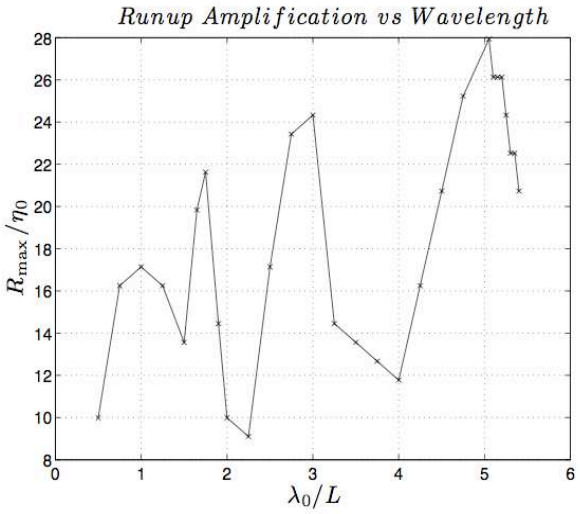

(b)

Fig. 10: (a) Transect of the Mentawai bathymetry. (b) Amplification ratio as a function of non-dimensional wavelength.

REFERENCES

Abramowitz, M and Stegun, IA (1965). *Handbook of Mathematical Functions*, Dover.

Agnon, Y and Mei, CC (1988). "Trapping and Resonance of Long Shelf Waves due to Groups of Short Waves," *J Fluid Mech*, Vol 195, pp 201-221.

Antuono, M and Brocchini, M (2007). "The Boundary Value Problem for the Nonlinear Shallow Water Equations," *Stud Appl Math*, Vol 119, pp 73-93.

Antuono, M and Brocchini, M (2010). "Solving the Nonlinear Shallow-Water Equations in Physical Space," *J Fluid Mech*, Vol 643, pp 207-232.

Brocchini, M and Peregrine, DH (1996). "Integral Flow Properties of the Swash Zone and Averaging," *J Fluid Mech*, Vol 317, pp 241-273.

Carrier, GF (1966). "Gravity Waves on Water of Variable Depth,"

J Fluid Mech, Vol 24, pp 641-659.

Carrier, GF and Greenspan, HP (1958). "Water Waves of Finite Amplitude on a Sloping Beach," *J Fluid Mech*, Vol 4, pp 97-109.

Dias, F and Milewski, P (2010). "On the Fully-Nonlinear Shallow Water Generalized Serre Equations," Phys Lett A, Vol 374, pp 1049-1053.

Didenkulova, I and Pelinovsky, E (2008) "Run-up of Long Waves on a Beach: The Influence of the Incident Wave Form," *Oceanology*, Vol 48, pp 1-6.

Dutykh, D and Dias, F (2009). "Energy of Tsunami Waves Generated by Bottom Motion," *Proc R Soc A*, Vol 465, pp 725-744.

Dutykh, D, Katsaounis, T and Mitsotakis, D (2011a). "Finite Volume Schemes for Dispersive Wave Propagation and Runup," *J Comput Phys*, Vol 230, pp 3035-3061.

Dutykh, D, Poncet, R and Dias, F (2011b). "The VOLNA code for the numerical modeling of tsunami waves: Generation, propagation and inundation," *Eur J Mech B/Fluids*, Vol 30, pp 598-615.

Fritz, HM, Kongko, W, Moore, A, McAdoo, B, Goff, J, Harbitz, C, Uslu, B, Kalligeris, N, Suteja, D, Kalsum, K, Titov, VV, Gusman, A, and Latief, H, Santoso, E, Sujoko, S, Djulkarnaen, D, Sunendar, H and Synolakis, C (2007). "Extreme Runup from the 17 July 2006 Java Tsunami," *Geophys Res Lett*, Vol 34, L12602.

Grataloup, GL and Mei, CC (2003). "Localization of Harmonics Generated in Nonlinear Shallow Water Waves," *Phys Rev E*, Vol 68, pp 026314.

Kajiura, K (1977) "Local Behaviour of Tsunamis," in *Waves on Water of Variable Depth*, *Lecture Notes in Physics* Vol. 64, pp 72-79

Keller, J and Keller, H (1964). "Water Wave Run-up on a Beach," ONR Research Report Contract No. NONR-3828(00).

Madsen, PA and Schaffer, HA (2010). "Analytical Solutions for Tsunami Runup on a Plane Beach: Single Waves, N-Waves and Transient Waves," *J Fluid Mech,* Vol 645, pp 27-57.

Madsen, PA, Fuhrman, DR and Schaffer, HA (2008). "On the Solitary Wave Paradigm for Tsunamis," J Geophys Res, Vol 113, pp C12012- C12034.

Munk, W, Snodgrass, F and Freeman, G (1964). "Long Waves on the Continental Shelf: An Experiment to Separate Trapped and Leaky Modes," *J Fluid Mech*, Vol 20, pp 529-554.

Neetu, S, Suresh, I, Shankar, R, Nagarajan, B, Sharma, R, Shenoi, S, Unnikrishnan, A and Sundar, D (2011). "Trapped Waves of the 27 November 1945 Makran Tsunami: Observations and Numerical Modeling," *Nat Hazards*, Vol 59, pp 1609-1618.

Pelinovsky, E and Mazova, RK (1992). "Exact Analytical Solutions of Nonlinear Problems of Tsunami Wave Run-up on Slopes with Different Profiles," *Nat Hazards*, Vol 6, pp 227-249.

Rabinovich, AB and Leviant, AS (1992). "Influence of Seiche Oscillations on the Formation of the Long-Wave Spectrum Near the Coast of the Southern Kuriles," *Oceanology*, Vol 32, pp 17-23.

Serre, F (1953). "Contribution à l' Etude des Ecoulements Permanents et Variables Dans les Canaux," *La Houille blanche*, Vol 8, pp 374–388 & 830–872.

Sorensen, R (1977). "*Basic Coastal Engineering"*, Springer, New York.

Stefanakis, TS, Dias, F and Dutykh, D (2011). "Local Run-up Amplification by Resonant Wave Interactions," *Phys Rev Lett*, Vol 107, pp 124502.

Synolakis, CE (1987). "The Runup of Solitary Waves," *J Fluid Mech,* Vol 185, pp 523-545.

Tadepalli, S and Synolakis, CE (1994). "The Run-up of N-Waves on Sloping Beaches," *Proc R Soc A*, Vol 445, pp 99-112.